Wave Generation Theory

Frigaard, Peter; Høgedal, Michael; Christensen, Morten

Publication date:
1993

Document Version
Publisher's PDF, also known as Version of record

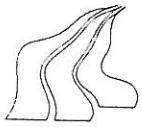

Wave generation theory

Peter Frigaard
Michael Høgedal
Morten Christensen

Hydraulics & Coastal Engineering Laboratory
Department of Civil Engineering
Aalborg University

June 1993

Contents

Chapter 1

Introduction

The intention of this manual is to provide some formulas and techniques which can be used for generating waves in hydraulic laboratories. Both long crested waves (2-D waves) and short crested waves (3-D waves) are considered.

"Les Appareils generateurs de houle en laboratorie" (Laboratory wave generating apparatus) by Biesel and Suquet was presented in the hydraulic journal "La Houille Blanche" in 1951, and marked the start of todays wave generating techniques. The paper presented the transfer functions between generator movement and generated wave field for a number of different wave generator types.

By controlling the movement of the wave generator it is possible to generate any desired wave field in a wave flume or in a wave basin. Present days direct current controlled step motors or oil valves enable together with PC installed Digital to Analog cards any user to control the wave generator and thereby the wave field.

In this handbook the Biésel Transfer Functions and the theory necessary for generating wave generator control signals are presented, together with a detailed description of the requirements for the wave generating system and how to use real-time programming in wave generation.

For convenience the handbook is divided into five chapters.

Chapter 2 describes the principles used for generating 2-D waves. The Biésel Transfer Function for 2-D waves is described. Three different techniques for generating control signals are outlined; that is the Random Phase Method, the Random Complex Spectrum Method and the White Noise Filtering Technique. Techniques to reduce the unwanted effects from free sub- and super harmonics by modifying the control signal are described in detail.

Chapter 3 describes the principles used for generating 3-D waves. The Biésel Transfer Function for 3-D waves is described. Control signal generation using the filter technique is described. Spurious waves, caused by the finite number of wave paddles, are described.

Chapter 4 describes how to use real-time programming on a small PC when generating waves.

Chapter 2

2-D Waves

This section introduces three mathematical techniques for generating 2 dimensional waves in a laboratory environment. The techniques are: the Random Phase Method, the Random Complex Spectrum Method and the White Noise Filtering Method. The pros and cons of the outlined techniques are discussed in detail in each section.
First a mathematical description of ocean waves and the general hydrodynamic considerations are listed.

2.1 Charachteristics of waves

Wind generated ocean waves are random in nature. Normally they are described mathematically as the summation of a large number of sinusoids. The amplitudes and phases of these sinusoids are determined by means of Fourier transformation of the surface elevation time series. The Fourier transform yields the frequency charachteristics of a given wave train. It is common practice to describe a wave train by means of its energy (variance) spectrum.

A mathematical formula is often used to describe the spectrum of a wave train. These mathematical formulas have been derived by fitting actual recorded wave data under various conditions. Spectral densities are given as a function of conditions (wind speed and fetch length) or statistics describing the sea state (significant wave height H_s and peak frequency f_p).
Different forms of the spectrum at its various generation stages have been obtained. Two such empirical spectra, the Pierson-Moskowitz and JONSWAP spectra, are given below. The former represents fully-developed sea states whereas the latter

represents conditions at which the fetch length of the wind is a limiting factor.

Pierson-Moskowitz type:

$$S_\eta(f) = \frac{\alpha g^2}{(2\pi)^4} f^{-5} exp\left(-0.74\left(\frac{f_0}{f}\right)^4\right)$$

where

$$\begin{aligned} \alpha &= 0.0081 \\ f_0 &= g\,(2\pi U_{19.5})^{-1} \end{aligned}$$

and $U_{19.5}$ denotes the wind speed 19.5 m above mean water level.

Pierson-Moskowitz type, parametrized:

$$S_\eta(f) = \frac{5}{16} H_s^2 f_p^4 f^{-5} exp\left(-\frac{5}{4}\left(\frac{f_p}{f}\right)^4\right)$$

Jonswap type:

$$S_\eta(f) = \frac{\alpha g^2}{(2\pi)^4} f^{-5} exp\left(-\frac{5}{4}\left(\frac{f}{f_m}\right)^{-4}\right) \gamma^{exp\left(-\frac{1}{2\sigma^2}\left(\frac{f}{f_m}-1\right)^2\right)}$$

where

$$\begin{aligned} \alpha &= 0.076\, x^{-0.22} \\ x &= g\, F\, U_{10}^{-2} \\ f_m &= \frac{3.5\, g\, x^{-0.33}}{U_{10}} \\ \sigma_f &= 0.07 \qquad f \le f_p \\ \sigma_f &= 0.09 \qquad f > f_p \\ \gamma &= 3.3 \end{aligned}$$

and U_{10} denotes the wind speed 10 m above mean water level.

Jonswap type, parametrized:

$$S_\eta(f) = \frac{1.4}{\gamma}\frac{5}{16} H_s^2 f_p^4 f^{-5} \gamma^\alpha exp\left(-\frac{5}{4}\left(\frac{f_p}{f}\right)^4\right)$$

$$\alpha = exp\left(-\frac{(f-f_p)^2}{2\sigma_f^2 f_p^2}\right)$$

where

$$\sigma_f = 0.10 \qquad f \leq f_p$$
$$\sigma_f = 0.50 \qquad f > f_p$$
$$\gamma = 3.3$$

Generation of irregular waves in laboratory environments combines the mathematical description of irregular waves presented above with the transfer function describing the relation between wave generator displacements and surface elevations for sinusoidal motions of the generator.
The derivation of this transfer function is given below.

2.2 Biésel Transfer Functions

"Les Appareils Generateurs de Houle en Laboratorie" presented by Biésel and Suquet in 1951 discussed and solved the analytical problems concerning a number of different wave generator types. For each wave maker type the paper presented the transfer function between wave maker displacement and wave amplitude in those cases where the analytical problem could be solved. The article therefore represented a giant step in wave generation techniques and found the basis for today's wave generation in hydraulics laboratories.

In this section the main results from Biésel and Suquet will be discussed, and the transfer function between wave amplitude and paddle displacement, The Biésel Transfer Function, for a piston type and a flap type wave maker will be presented.

In figure 2.1 the definitions used in the following calculations are presented for a piston-type wave maker.

In figure 2.2 the fundamental hydrodynamic problem is shown in mathematical terms. The velocity potential, φ, is introduced, which implies that the flow is assumed irrotational and incompressible, in other words a potential flow.

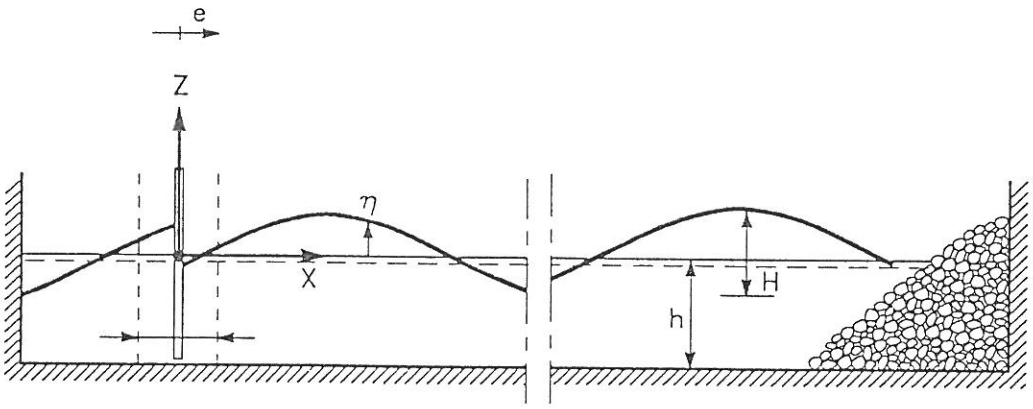

Figure 2.1: Definition sketch of flume with piston-type wave maker. e = e(z,t) = displacement of wave paddle. S = S(z) = stroke of wave paddle. $\eta = \eta(x,t)$ = surface elevation. H = wave heigth far away from the wave maker. h = water depth, (assumed to be constant).

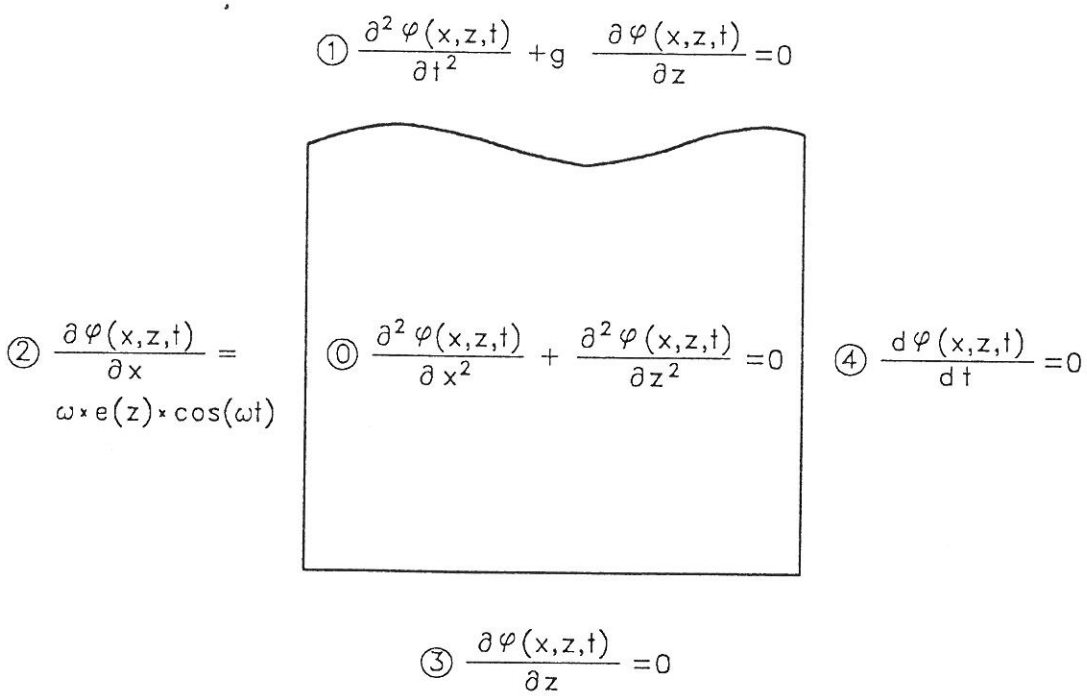

Figure 2.2: Partial differential equation (PDE), and boundary conditions (BC).

In figure 2.2 the equations express:

0. Laplace equation. Basic equation for potential flow.
1. All water particles at the free surface remain at the free surface (kinematic B.C.). Free surface is at constant pressure (dynamic B.C.).
2. The water accompanies the wave paddle, which is displaced as a sine $e(z,t) = \frac{S(z)}{2}\sin(\omega t)$.
3. The bottom is impermeable.
4. The propagating wave is of constant form.

Solution, with respect to φ, of the boundary value problem presented in figure 2.2 can be divided into 3 steps:

A. Solving the homogeneous problem. That is PDE with BC 1,2 and 3. BC 2 with right side equal to zero.

B. Finding a particular solution satisfying PDE and BC 1, 2 and 3.

C. Determining the final solution, as a linear combination of the homogeneous solution and the particular solution, that satisfies BC 4.

The main results from each step (linearised BC) are listed below:

A. Homogeneous solution is any linear combinations of functions of the form:

$$\varphi_H(x,z,t) = A_H \cdot \cos(k_i x) \cdot \cosh(k_i(z+h)) \cdot \cos(\omega_i t - \psi_0)$$

where A_H and ψ_0 are arbitrary constants and k is the solution to the dispersion relation:

$$\omega^2{}_i = k_i \cdot g \cdot \tanh(k_i h)$$

B. Particular solution.

$$\varphi_P(x,z,t) = \left(\sum_{n=0}^{\infty} c_n \varphi_n\right) \cos(\omega t)$$

where

$$\varphi_0 = \frac{\omega_i}{k_0} \cosh\left(k_0(z+h)\right) \cdot \sin\left(k_0 x\right)$$

$$c_0 = 2 \cdot k_0 \frac{\int_{-h}^{0} e(z) \cdot \cosh\left(k_0\left(z+h\right)\right) \cdot dz}{\sinh\left(k_0 h\right) \cdot \cosh\left(k_0 h\right) + k_0 h}$$

$$\varphi_n = -\frac{\omega}{k_n} \cos\left(k_n\left(z+h\right)\right) \cdot e^{-k_n x} \quad , \quad n > 0$$

$$c_n = 2 \cdot k_n \frac{\int_{-h}^{0} e(z) \cdot \cos\left(k_n\left(z+h\right)\right) \cdot dz}{\sin\left(k_n h\right) \cdot \cos\left(k_n h\right) + k_n h} \quad , \quad n > 0$$

where k_0 is the solution to the dispersion relation:

$$\omega^2{}_i = k_i \cdot g \cdot \tanh\left(k_i h\right)$$

and k_1 is the first positive solution (n=1) to

$$\omega^2 = -k_n \, g \, tan\left(k_n h\right)$$

k_2 the second and so forth.

C. Determining the final solution.
Now, requiring BC 4 to be satisfied far away from the wavemaker the only velocity potential $\varphi = \varphi_H + \varphi_P$ that satisfy the PDE and BC 1 to 4 is found to be, omitting index 0 :

$$\varphi(x,z,t) = \frac{\omega}{k} \cdot c \cdot \cosh\left(k\left(z+h\right)\right) \cdot \sin(\omega t - kx) + \sum_{n=1}^{\infty} c_n \cdot \frac{\omega}{k_n} \cdot \cos\left(k_n\left(z+h\right)\right) \cdot e^{-k_n x} \cdot \cos(\omega t)$$

The surface elevation $\eta(x,t)$ in the generated wave field is calculated by:

$$\eta(x,t) = \int \frac{\partial \varphi(x,z,t)}{\partial z} dt \quad , \quad z = 0$$

that is

$$\eta(x,t) = c \cdot \sinh(kh) \cos(\omega t - kx) + \sum_{n=1}^{\infty} c_n \sin\left(k_n h\right) e^{-k_n \cdot x} \sin(\omega t)$$

The first term in the function expresses the velocity potential at infinity, by Biésel called the far-field solution, while the second term is the near-field solution. The first term describes the generated progressive wave, while the second describes the standing waves which decreases with the distance from the wavemaker.

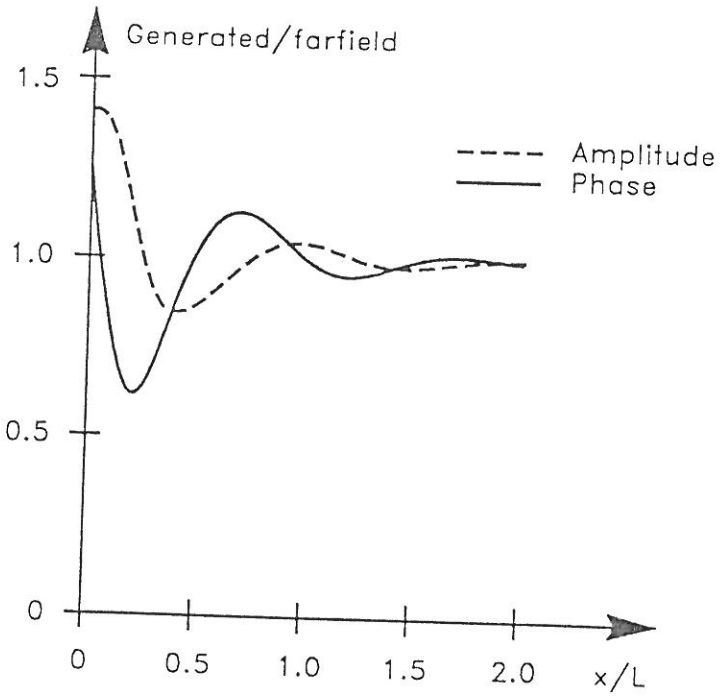

Figure 2.3: Wave amplitude and phase of the generated wave field relative to the far-field solution. Water depth = 0.7 m and wave period = 0.7 sec

In general only the far-field solution is considered. As the displacement, e, of the wave generator is defined by

$$e(z,t) = \frac{S(z)}{2}\sin(\omega t)$$

The far-field surface elevation is seen to be phase shifted $\frac{\pi}{2}$ relative to the displacement of the wave generator. The "disturbance" from the near-field solution will in a distance of 1-2 wave lengths from the wavemaker be less than 1% of the far-field solution. See figure 2.3

It is now straight forward to calculate the Biésel Transfer Function for any wave maker as long as the stroke, $S(z)$, of the paddle can be described. As stated by Biésel, it is necessary to require that $S(z)$ and its first two(three) derivatives are limited for $-h < z < 0$.

In figure 2.4 to 2.7 are listed some solutions for the piston-type and the hinged-type wave maker. The reader can with little effort add any wave maker to this list. The Biésel Transfer Function is in these figures defined as the ratio between the far-field wave height, H and the stroke of the paddle for $z = 0$, denoted S_0.

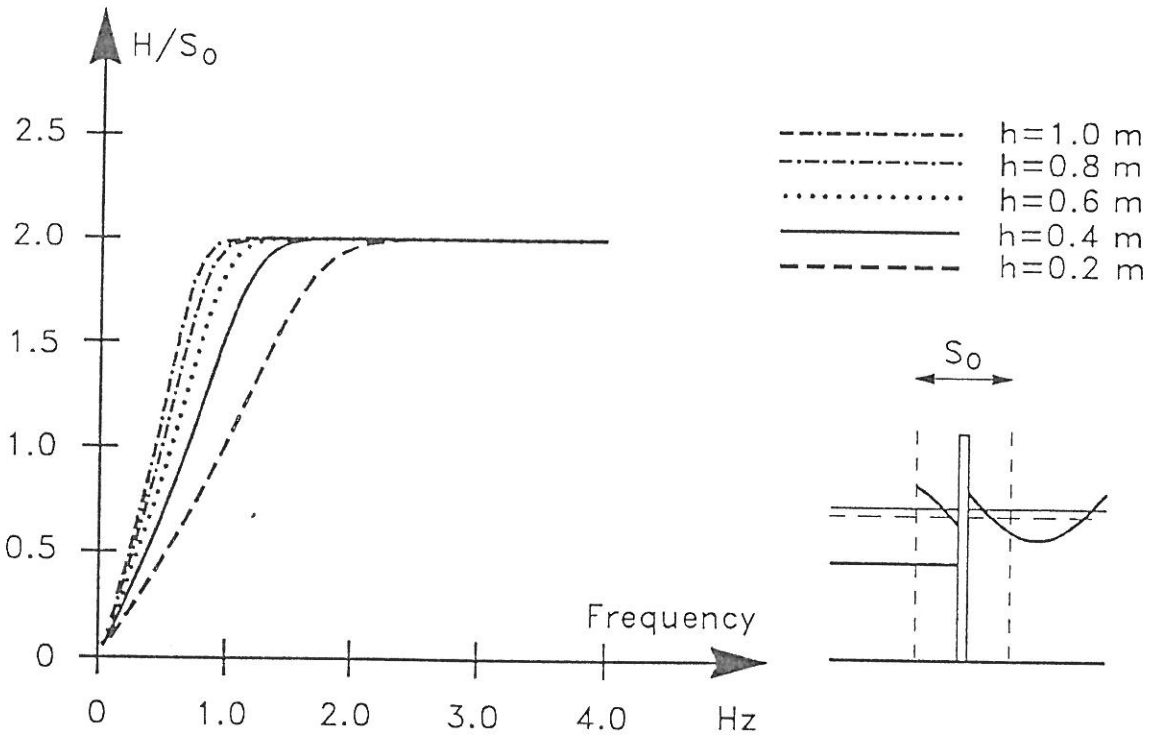

$$S(z) = S_0.$$

$$\frac{H}{S_0} = \frac{2\sinh^2(kh)}{\sinh(kh)\cosh(kh) + kh}$$

Figure 2.4: Far field Biesel Transfer Function for piston-type wave maker.

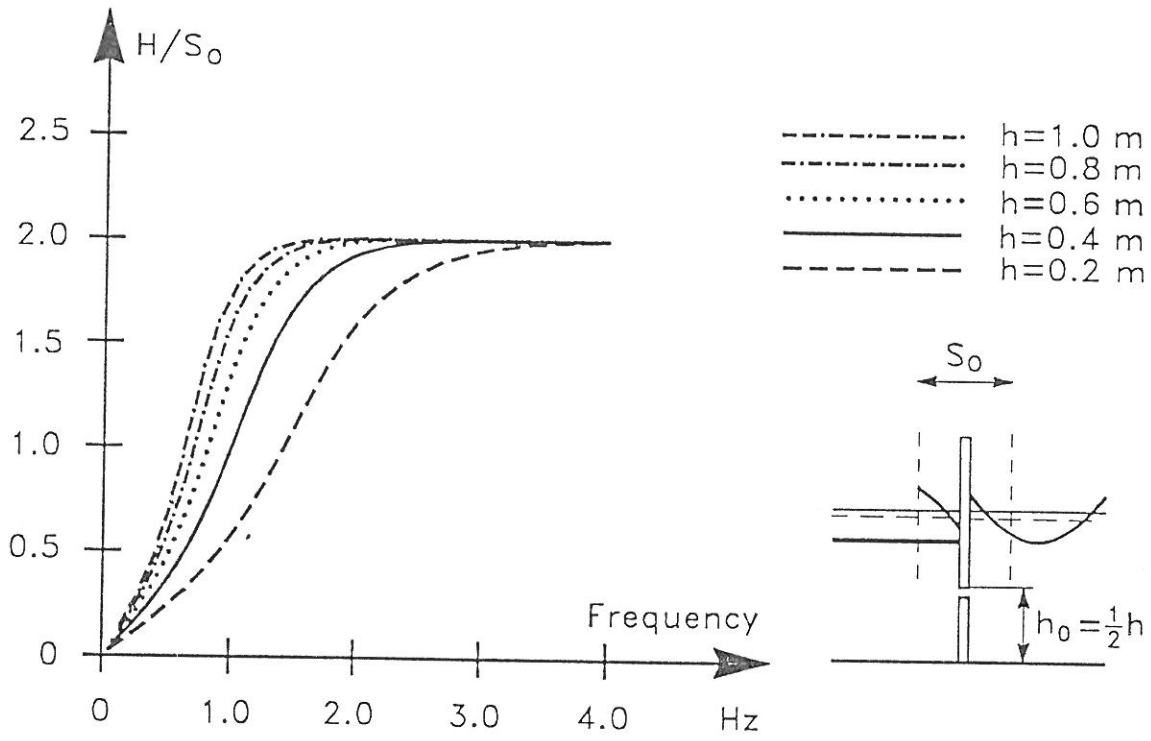

$$S(z) = S_0 \ , \quad (z+h) > h_0$$
$$S(z) = 0 \ , \quad (z+h) < h_0$$
$$\frac{H}{S_0} = \frac{2\sinh^2(kh) - 2\sinh(kh_0)\sinh(kh)}{\sinh(kh)\cosh(kh) + kh}$$

Figure 2.5: Far field Biesel Transfer Function for elevated piston-type wave maker.

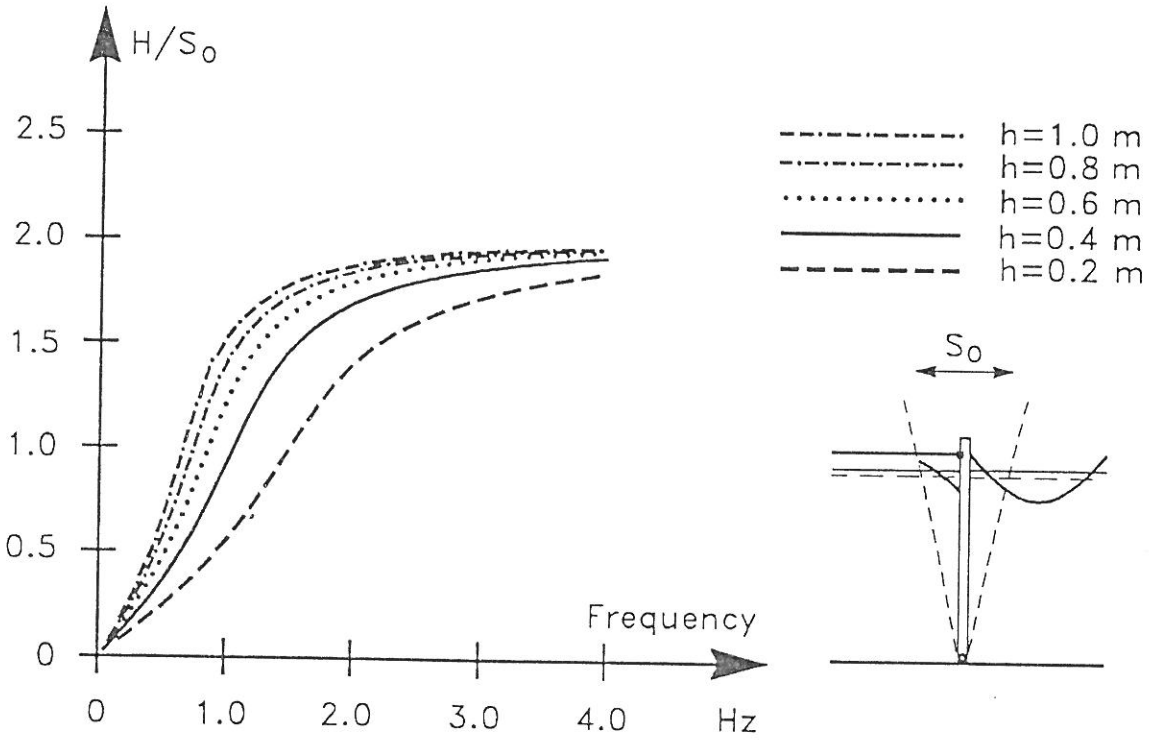

$$S(z) = \frac{S_0}{h} \cdot (h + z)$$

$$\frac{H}{S_0} = \frac{2 \sinh(kh)\,(1 - \cosh(kh) + kh \sinh(kh))}{kh\ (\sinh(kh)\cosh(kh) + kh)}$$

Figure 2.6: Far field Biesel Transfer Function for hinged-type wave maker.

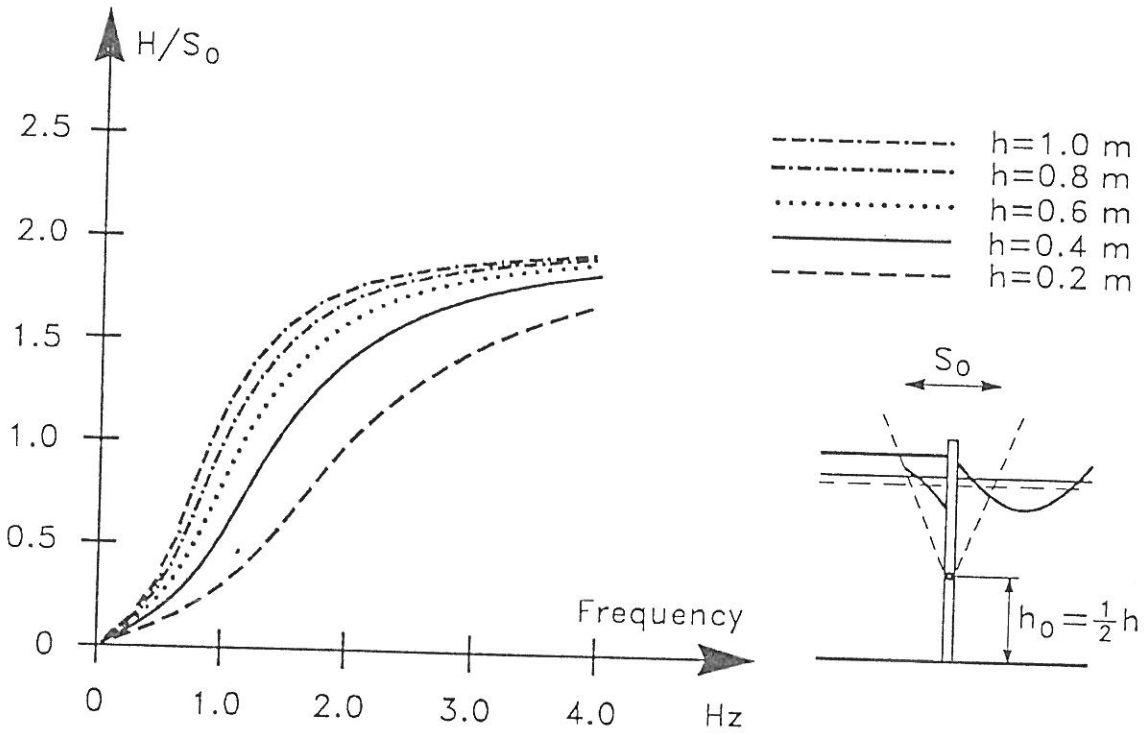

$$S(z) = S_0 \cdot \frac{h+z-h_0}{h-h_0} \quad , \quad (z+h) > h_0$$

$$S(z) = 0 \quad , \quad (z+h) < h_0$$

$$\frac{H}{S_0} = \frac{2}{k\,(h-h_0)} \left[\frac{\sinh(kh)\,((h-h_0)\,k\,\sinh(kh) - \cosh(kh) + \cosh(kh_0))}{\sinh(kh)\,\cosh(kh) + kh} \right]$$

Figure 2.7: Far field Biesel Transfer Function for elevated hinged-type wave maker.

2.3 Wave Generation Techniques

A number of techniques for reproducing irregular wave trains with specified characteristics have been developed. In general, these wave generation techniques fall into two categories: deterministic and non-deterministic techniques.

Deterministic wave generation techniques produce wave trains of finite duration which match the specified charachteristics (the target wave spectrum) exactly.

Non-deterministic (probabilistic) techniques produce wave trains which only match the specified charachteristics within the bounds of probability. Thus, a single generated wave train will not match the target wave energy spectrum. However, the average energy spectrum will approach the target energy spectrum as the number of generated wave trains increases.

In the following, three wave generation techniques will be presented.

The Random Phase Method and the Random Complex Spectrum Method simulate random waves in the frequency domain with subsequent use of the FFT-algorithm in order to obtain the time domain representation of the wave train. The Random Phase Method is a deterministic wave generation technique whereas the Random Complex Spectrum Method is non-deterministic. Both techniques were developed by Rice (1944) and their application to random wave generation (linear and non-linear) was described by Tuah and Hudspeth (1982).

The White Noise Filtering Method simulates random waves in the time domain by means of digital filtering. This method is non-deterministic. It was described by Nunes (1981).

In nature, non-linear interaction between individual wave components in irregular wave trains give rise to so-called group bounded long waves (Ottesen-Hansen, 1978). In physical model tests, correct reproduction of these waves is often essential. Therefore, methods for correct reproduction of group bounded long waves will be given.

2.4 Random Phase Method

In the Random Phase Method, wave trains are generated by combining the discrete amplitude wave spectrum corresponding to the target wave energy spectrum with a random phase spectrum synthesized from a random number generator. This yields the Fourier Transform of a time series with the desired discrete power spectrum.

The corresponding time series is obtained by Inverse Fourier Transformation.

The steps of calculating a time series using the Random Phase Method are:

1. Define a target wave energy density spectrum. This might be from measurements in nature or from calculations using deterministic expressions like the Pierson-Moskowitz formulation of the spectral density S_η:

$$S_\eta(f) = \frac{5}{16} H_s^2 f_p^4 f^{-5} exp\left(-\frac{5}{4}\left(\frac{f_p}{f}\right)^4\right)$$

where

H_s = significant wave height
f_p = peak frequency
f = frequency

2. Choose the sample frequency, f_s and the resolution of the spectrum (half the number of Fourier components) N. This yields a frequency domain resolution of $\Delta f = \frac{f_s}{N}$. Calculate the discrete wave energy spectrum $\sigma_\eta^2(f_i)$:

$$\sigma_\eta^2(f_i) = S_\eta(i \cdot \Delta f) \cdot \Delta f$$

3. Determine the discrete paddle-displacement energy spectrum.
The far field transfer function for small amplitude regular waves was given by Biésel (1951) in the following form for piston wave paddles:

$$\frac{H}{S_0} = \frac{2 \sinh^2(kh)}{\sinh(kh) \cosh(kh) + kh}$$

where

H = wave height
k = wave number $\left(\frac{2\pi}{L}\right)$
h = water depth
S_0 = stroke of the piston

When the water depth is known it is possible to calculate the Biésel transfer function.

It is now possible to determine the discrete paddle-displacement energy spectrum, $\sigma_x^2(f_i)$:

$$\sigma_x^2(f_i) = \frac{\sigma_\eta^2(f)}{\left(\frac{2 \sinh^2(kh)}{\sinh(kh) \cosh(kh)+kh}\right)^2}$$

note that k is a function of frequency.

4. Calculate the N complex Fourier coefficients $C = A + i \cdot B$ by picking a random phase, $\varphi(f)$, between 0 and 2π for all frequencies smaller than the Nyquist frequency, $f_n = f_s/2$:

$$A_i = \cos(\varphi(f_i)) \cdot \sqrt{\sigma_x^2(f_i)}/\sqrt{2}$$
$$B_i = \sin(\varphi(f_i)) \cdot \sqrt{\sigma_x^2(f_i)}/\sqrt{2}$$

Mirror the N Fourier components into the Nyquist frequency f_n in order to obtain a hermitian Fourier Transform, i.e.:

$$C_{N+i} = C^*_{N-i+1} \ , \ i = 1..N$$

where * denotes complex conjugate.

5. Apply the inverse Fourier Transform (IFFT) and calculate the time series of the control signal for the wave paddle (the real parts of the inverse Fourier Transform is the time series, the imaginary parts are zero due to the fact that the Fourier Transform is hermitian).

6. Use oversampling in order to get a better discretization of the control signal.

Figures 2.8-2.12 illustrate the procedure described above applied to a specific example.

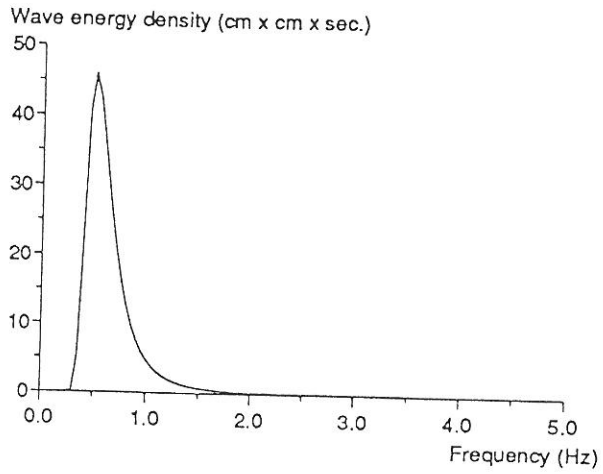

Figure 2.8: Example of calculated model wave energy density spectra $S_f(f)$ using the PM-spectra with $H_s = 0.16\ m, f_p = 0.5\ Hz$.

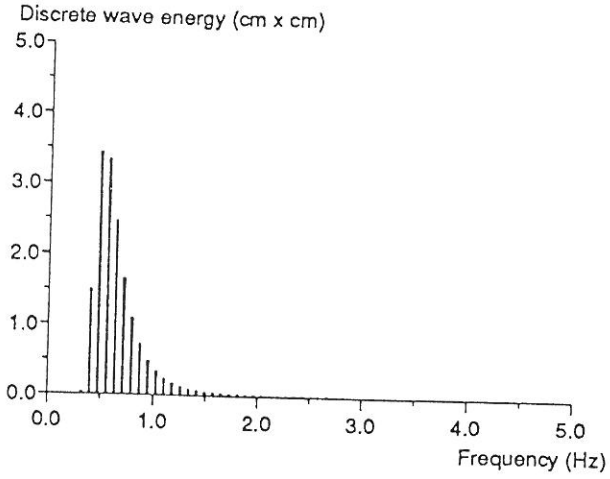

Figure 2.9: Example of discrete wave energy spectrum σ_η^2. PM-spectrum. $H_s = 0.16\ m, f_p = 0.5\ Hz, f_s = 5\ Hz, N = 32$. For practical use N must be much larger.

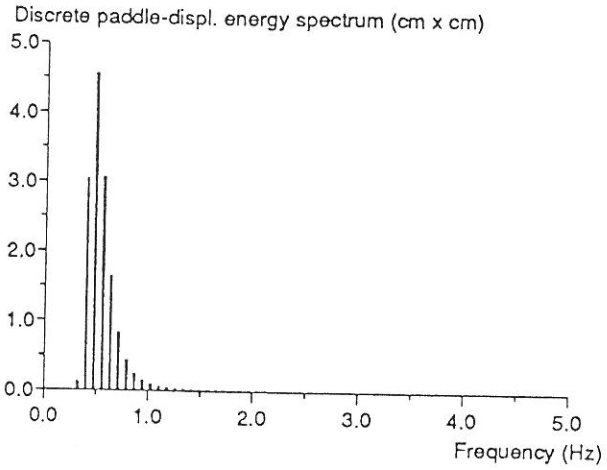

Figure 2.10: Discrete paddle displacement energy spectrum σ_x^2. Example using PM-spectrum with $H_s = 0.16\ m$, $f_p = 0.5\ Hz$, $f_s = 5\ Hz$, $N = 32$, $h = 0.70\ m$ and piston wave generator.

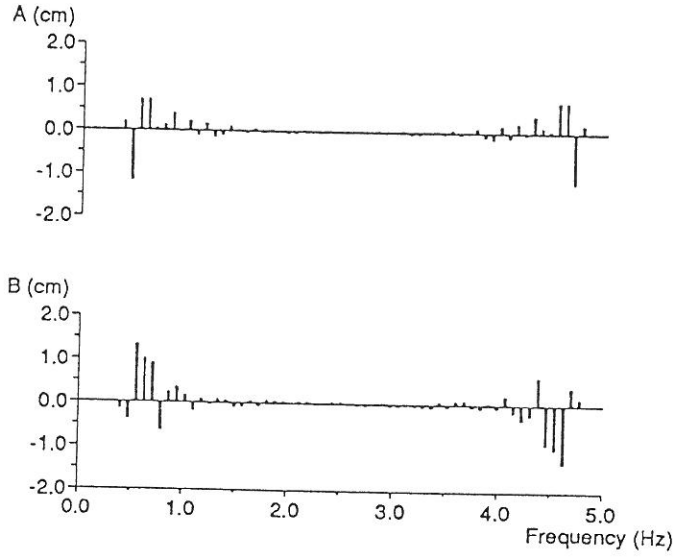

Figure 2.11: Real and imaginary parts of hermitian Fourier Transform. Example using PM-spectrum with $H_s = 0.16\ m$, $f_p = 0.5\ Hz$, $f_s = 5\ Hz$, $N = 32$, $h = 0.70\ m$ and piston wave generator.

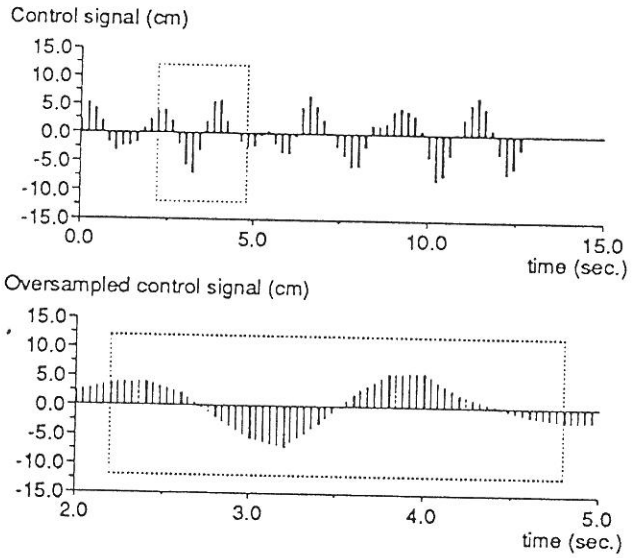

Figure 2.12: Paddle displacement time series. Example using PM-spectrum with $H_s = 0.16\ m$, $f_p = 0.5\ Hz$, $f_s = 5\ Hz$, $N = 32$, $h = 0.70\ m$ and piston wave generator.

The Random Phase Method is a deterministic wave generation method, i.e. the power spectrum of the generated wave train is identical to that of the target wave power spectrum over the length of the time series. This means that two different realizations with different spectral properties can be directly compared.

The length of the time series is only limited by the capacity of the computer performing the Fourier transform, but even with todays technology the computing time will be very significant for long time series.

Often a number of relatively short time series, say 5-10 minutes in length, calculated by means of the Random Phase Method are connected substituting a long realization in order to save computing time. This method is very efficient for pilot testings, calibration of wave generators, measurements of reflections etc.

However, for long simulations, where the right variations in the spectral distribution are required, one long time series must be used in order to get the right variability of the spectra for short samples. Alternatively another wave generation technique i.e. the Filtered White Noise technique should be used.

2.5 Random Complex Spectrum Method

The Random Complex Spectrum Method is a non-deterministic wave generation technique which produces time series with Gaussian distributed amplitude spectra.

The technique is rather similar to the Random Phase Method. However, When the Random Complex Spectrum Method is applied, the real and imaginary components of the complex Fourier coefficients (sec. 2.3, item 4) are determined as:

$$\begin{aligned} A_i &= G_j \cdot \sqrt{\sigma_x^2(f_i)}/\sqrt{2} \\ B_i &= G_{j+1} \cdot \sqrt{\sigma_x^2(f_i)}/\sqrt{2} \end{aligned}$$

where G is a normally distributed random variable with zero mean and a standard deviation of $\sigma = 1$.

This method has the same limitations as the Random Phase Method: the length of the time series is limited by the capacity of the computer performing the Fourier transformation. An equivalent method which is not subject to this limitation will be described in the following section.

2.6 White Noise Filtering Method

The technique is based on the use of digital filters. Socalled FIR-filters (Finite Impulse Response filters) are applied (Karl, p. 165).
In essence, a digital filter is designed by computing the time domain terms h_i called filter coefficients (or the filter operator), for use in convolving with the input data in order to achieve a specific frequency response.

The surface elevation time series $\eta(t)$ is obtained by generating a white noise signal $W(t)$ (samples from a unit normal random variable) which is convolved with a filter operator determined by Inverse Fourier Transformation of a discrete frequency response function corresponding to the discrete target wave energy spectrum (the surface elevation filter). The input/output relation of this filter is given by the discrete convolution integral:

$$\eta_j = \sum_{i=0}^{2 \cdot N-1} h_i \cdot W_{j-i}$$

where $2 \cdot N$ denotes the number of filter coefficients.

To determine the corresponding wave paddle displacement time series, the surface elevation time series is convolved with another filter operator obtained by Inverse Fourier Transformation of a frequency response function corresponding to the inverse of the far field Biesel transfer function (the Biesel filter).

Designing the surface elevation filter can be divided into 6 steps:

1. The desired wave power spectrum is defined.

2. The wave power spectrum is discretized in N components.

3. For each component, a phase Φ_i is chosen as

$$\Phi_i = \begin{cases} 0 & \text{if i is even} \\ \pi & \text{if i is odd} \end{cases}$$

   This phase removes the phase shift introduced by the filter delay. For wave generation removing the phase shift is unnessecary. However, it is of importance in other applications.

4. Determine the value of the frequency response function H corresponding to each component i (frequency sampling)

$$H(f_i).re = cos(\Phi_i)\sqrt{\sigma_\eta^2(f_i)}/\sqrt{2}$$

$$H(f_i).im = sin(\Phi_i)\sqrt{\sigma_\eta^2(f_i)}/\sqrt{2}$$

H specifies the desired frequency response of the surface elevation filter.

5. Mirror the discrete frequency responce function into the nyquist frequency to obtain a Hermitian discrete frequency response function , i.e.

$$H(f_n + f_i) = H^*(f_n - f_i)$$

6. Compute the Inverse Fourier Transform of the frequency response function to produce the filter operator (the real parts of the IFT are the filter coefficients, the imaginary parts are zero due to the fact that H is hermitian).

The Biesel filter is designed by proceeding from step 3 and determining the discrete values of the frequency response function as

$$H(f_i).re = cos(\Phi_i)\frac{1}{K_f(f_i)}$$
$$H(f_i).im = sin(\Phi_i)\frac{1}{K_f(f_i)}$$

where K_f denotes the far field Biesel transfer function.
The phase Φ_i is chosen as $-\pi/2$ in order to eliminate the phase shift between flap displacements and surface elevations.

Figures 2.13-2.17 illustrate the White Noise Filtering Method applied to a specific example.

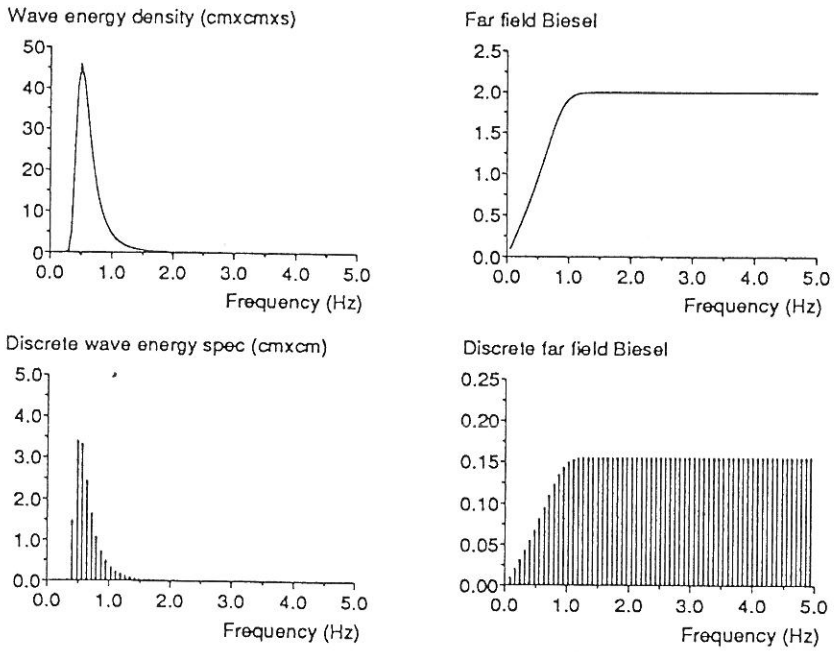

Figure 2.13: Discretization of wave energy spectrum (left) and Biesel far field transfer function (right). Example using the PM-spectra with $H_s = 0.16\ m$, $f_p = 0.5\ Hz$, $f_s = 5Hz$, $N = 32$ $h = 0.70\ m$ and piston wave generator.

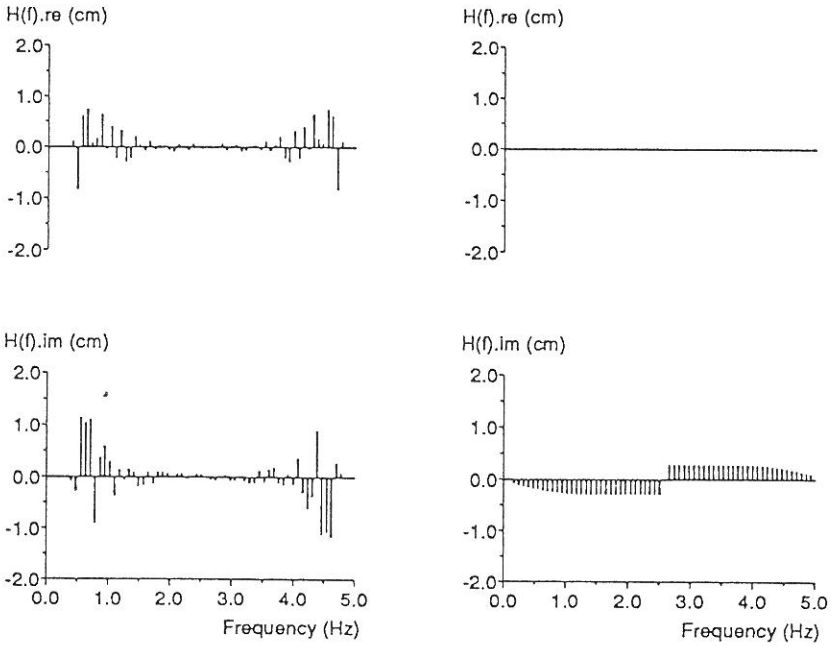

Figure 2.14: Discrete complex frequency response functions corresponding to surface elevation filter operator (left) and Biesel filter operator (right). Example using the PM-spectra with $H_s = 0.16\ m, f_p = 0.5\ Hz,\ f_s = 5Hz,\ N = 32\ h = 0.70\ m$ and piston wave generator.

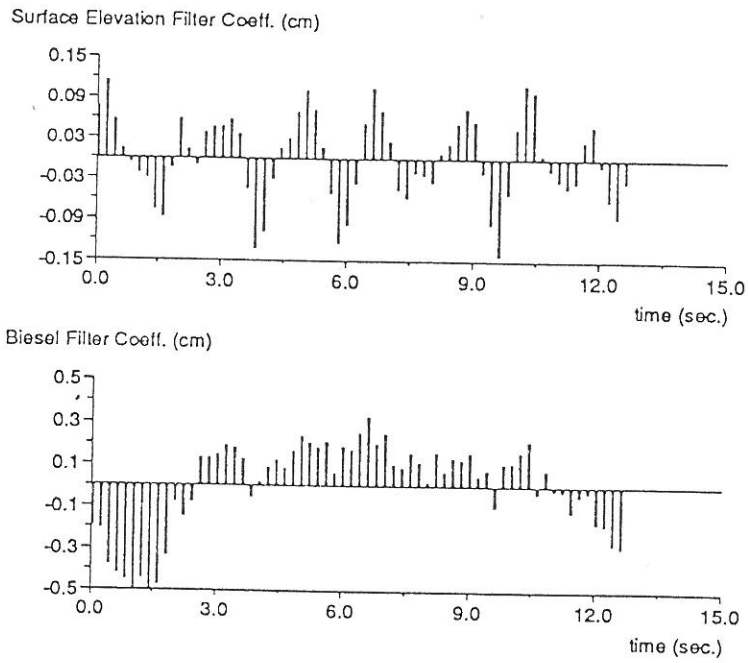

Figure 2.15: Surface elevation filter operator (left) and Biesel filter operator (right) obtained by means of InvFFT of complex frequency response functions. Example using the PM-spectra with $H_s = 0.16\ m, f_p = 0.5\ Hz$, $f_s = 5Hz$, $N = 32$ $h = 0.70\ m$ and piston wave generator.

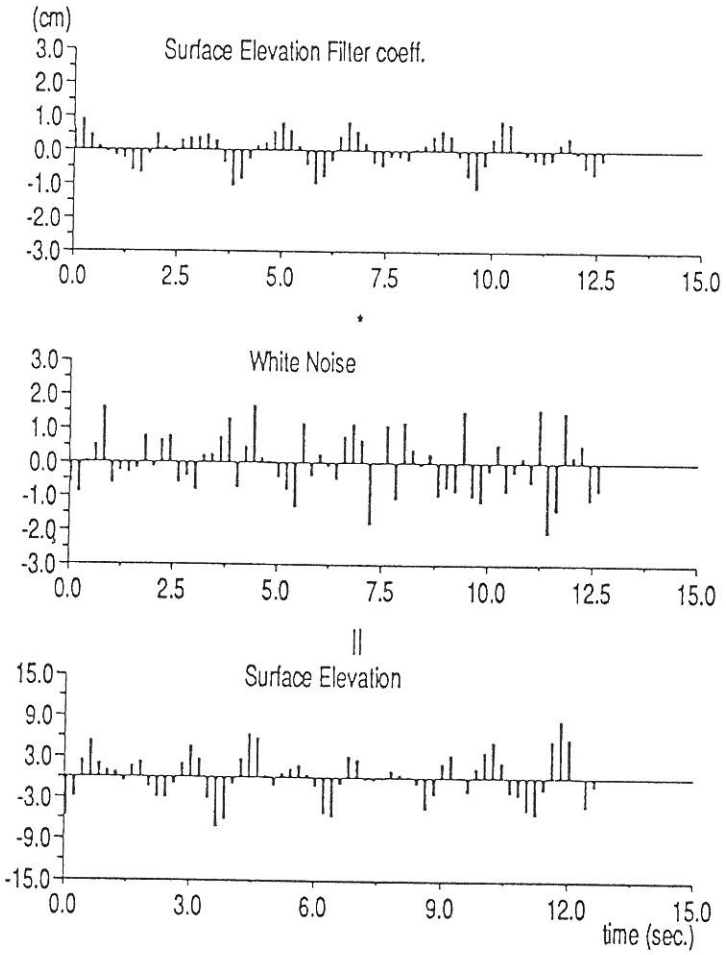

Figure 2.16: Surface elevation time series obtained by convolving the surface elevation filter operator with white noise time series. Convolution denoted by *. Example using the PM-spectra with $H_s = 0.16\ m, f_p = 0.5\ Hz, f_s = 5Hz, N = 32$ $h = 0.70\ m$ and piston wave generator.

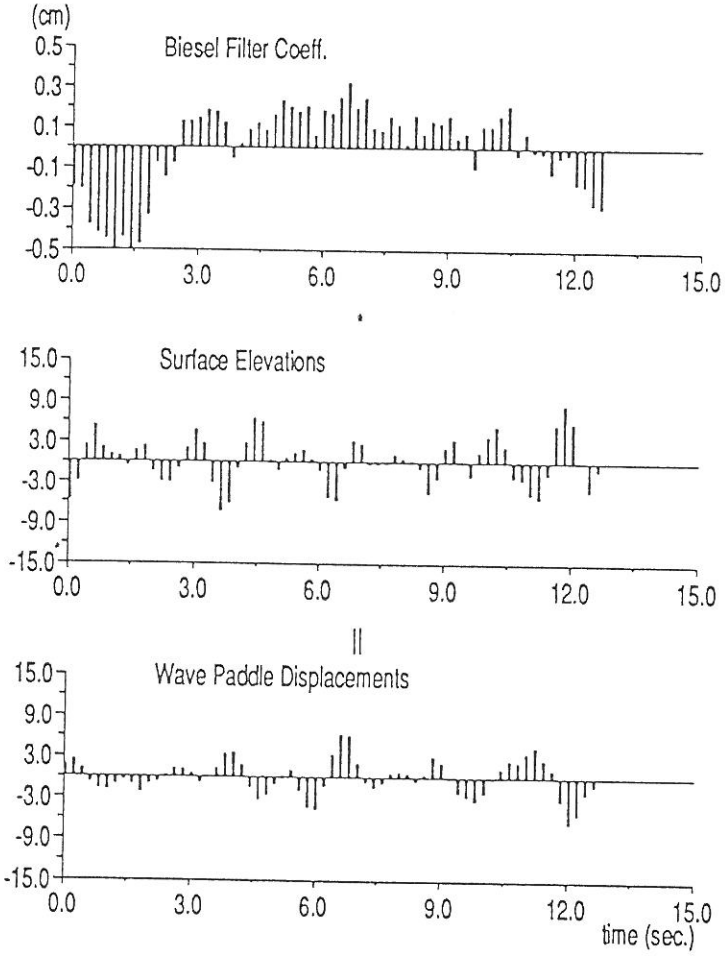

Figure 2.17: Wave paddle displacement time series obtained by convolving the Biesel filter operator with the surface elevation time series. Convolution denoted by *. Example using the PM-spectra with $H_s = 0.16\ m, f_p = 0.5\ Hz$, $f_s = 5Hz$, $N = 32$, $h = 0.70\ m$ and piston wave generator.

2.7 Bounded Long Waves

Non-linear interaction between individual wave components in irregular wave trains give rise to so-called group bounded long waves. These waves are of second order and therefore they cannot be reproduced by means of the linear (first order) wave generation theory presented by Biesel. Consequently, socalled spurious long wave components will occur when a first order paddle displacement signal is applied to the wave generator. The prescense of spurious long waves (free long waves) in physical model tests often leads to unrealistic responses of the test structures because of the dominant influence of the long waves on e.g. mooring forces and slow-drift oscillations.

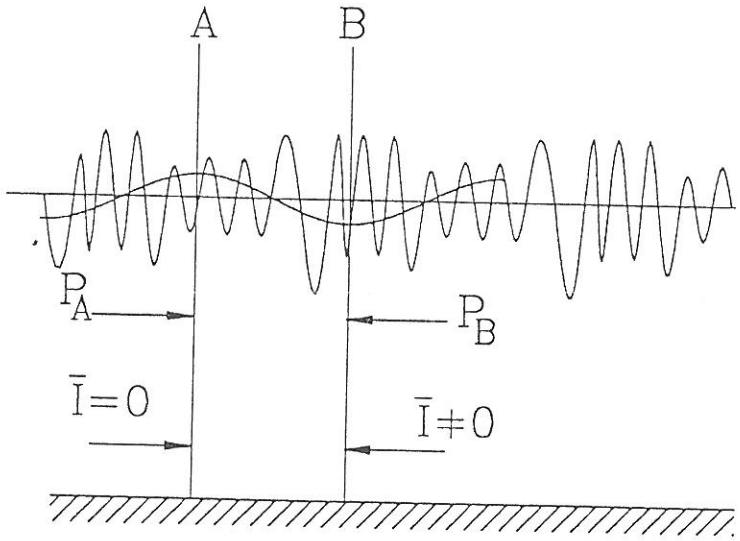

Figure 2.18: Wave group with bounded long wave.

The physical reason for the prescense of bounded long waves in natural wave trains is the "wave pressure force" or with another name the "wave reaction force" described by Fredsøe (1990). Considering the time averaged equation of momentum (Figure 2.18) we see that force equilibrium (total force (F) = pressure force (P) + momentum force (I)) only can be fulfilled when $P_A > P_B$. This yields the bounded long wave.

The problem of correctly reproducing the bounded long waves in physical model tests was solved by Sand (1982). By means of a perturbation analysis of the Laplace equation correct to second order, he derived the second order piston positions for

correct reproduction of the bounded long waves.

In the following, the results derived by Sand are outlined.

Both the calculations of second order long waves and second order piston positions are based on a Fourier decomposition of the first order wave train.
The long wave elevations $\zeta(t)$ are determined as the sum of the terms arising from interaction between individual components in the first order wave train

$$\zeta(t) = \sum_{n-m=1}^{\infty} \sum_{m=m^*}^{\infty} \zeta_{nm}(t), \quad m^* = \frac{\omega^*}{\omega_0}$$

where ω_0 is the frequency interval in the Fourier decomposition and ω^* is the lowest frequency in the first order spectrum.

Consider a pair of regular wavelets with frequencies ω_n and ω_m. Such a pair of wavelets constitutes a regular wave group, i.e.

$$\begin{aligned}\eta_{nm} &= \eta_n + \eta_m \\ &= a_n \cos(\omega_n t - k_n x) + b_n \sin(\omega_n t - k_n x) \\ &\quad + a_m \cos(\omega_m t - k_m x) + b_m \sin(\omega_m t - k_m x)\end{aligned}$$

The second order long wave generated by this wave group becomes

$$\begin{aligned}\frac{\zeta_{nm}}{h} &= G_{nm} h \left[\left(\frac{a_n a_m + b_n b_m}{h^2} \right) \cos(\Delta\omega_{nm} t - \Delta k_{nm} x) \right. \\ &\quad \left. + \left(\frac{a_m b_n - a_n b_m}{h^2} \right) \sin(\Delta\omega_{nm} t - \Delta k_{nm} x) \right]\end{aligned}$$

where

$$\begin{aligned}\Delta\omega_{nm} &= \omega_n - \omega_m \\ \Delta k_{nm} &= k_n - k_m\end{aligned}$$

and the transfer function G_{nm} is given by

$$\begin{aligned}G_{nm} h &= \left[\frac{4\pi^2 D_n D_m \Delta k_{nm} h \cosh(\Delta k_{nm} h)}{\cosh(k_n h + k_m h) - \cosh(\Delta k_{nm} h)} - 2\pi^2 (D_n - D_m)^2 \Delta k_{nm} h \right. \\ &\quad \left. + \frac{\Delta k_{nm} h (D_n - D_m)(k_n h D_m + k_m h D_n) \coth(\Delta k_{nm} h)}{2_n D_m} \right] \\ &\quad / \left[4\pi^2 (D_n - D_m)^2 \coth(\Delta k_{nm} h) - \Delta k_{nm} h \right]\end{aligned}$$

where

$$D_n = \sqrt{h/g}\ \cdot \omega_n/2\pi$$
$$D_m = \sqrt{h/g}\ \cdot \omega_m/2\pi$$

The second order piston positions for correct reproduction of the group bounded long waves given above are

$$X^{(2)}(t) = \sum_{n-m=1}^{\infty} \sum_{m=m^*}^{\infty} X^{(2)}_{nm}(t), \quad m^* = \frac{\omega^*}{\omega_0}$$

where

$$\frac{X^{(2)}_{nm}}{h} = \left[\left(\frac{a_n b_m - a_m b_n}{h^2}\right) F_1 h + \left(\frac{a_n a_m + b_n b_m}{h^2}\right) F_{23} h\right] \cos(\Delta\omega_{nm} t) + \left[\left(\frac{a_n a_m + b_n b_m}{h^2}\right) F_1 h + \left(\frac{a_m b_n - a_n b_m}{h^2}\right) F_{23} h\right] \sin(\Delta\omega_{nm} t)$$

where the transfer function F_1 is given by

$$F_1 h = F_{11} h^{'} + F_{12} h$$

in which

$$F_{11} h = \frac{G_{nm} h \Delta k_f h (\Delta k_{nm} h - \Delta k_f h) \sinh(\Delta k_{nm} h + \Delta k_f h) + (\Delta k_{nm} h + \Delta k_f h) \sinh(\Delta k_{nm} h - \Delta k_f h)}{2((\Delta k^2_{nm} h^2 - \Delta k^2_f h^2) \sinh(\Delta k_{nm} h) \sinh(\Delta k_f h)}$$

and

$$F_{12} h = \frac{f_m \Delta k_f h k_m h (1 + G_n) \left[\delta k^-_m h \sinh(\delta k^+_m h) + \delta k^+_m h \sinh(\delta k^-_m h)\right]}{\Delta f 8 (k^2_m h^2 - \Delta k^2_f h^2) \sinh(\Delta k_f h) \sinh(k_m h) \tanh(k_n h)} + \frac{f_m \Delta k_f h k_n h (1 + G_m) \left[\delta k^-_m h \sinh(\delta k^+_m h) + \delta k^+_m h \sinh(\delta k^-_m h)\right]}{\Delta f 8 (k^2_n h^2 - \Delta k^2_f h^2) \sinh(\Delta k_f h) \sinh(k_n h) \tanh(k_m h)}$$

where the free long wave number , Δk_f is derived from the dispersion relation

$$(\Delta\omega_{nm})^2 = g \Delta k_f \tanh(\Delta k_f h)$$

and

$$\delta k^+_m = k_m + \Delta k_f$$
$$\delta k^-_m = k_m - \Delta k_f$$

The transfer function $F_{23} h$ is negligible relative to $F_1 h$.

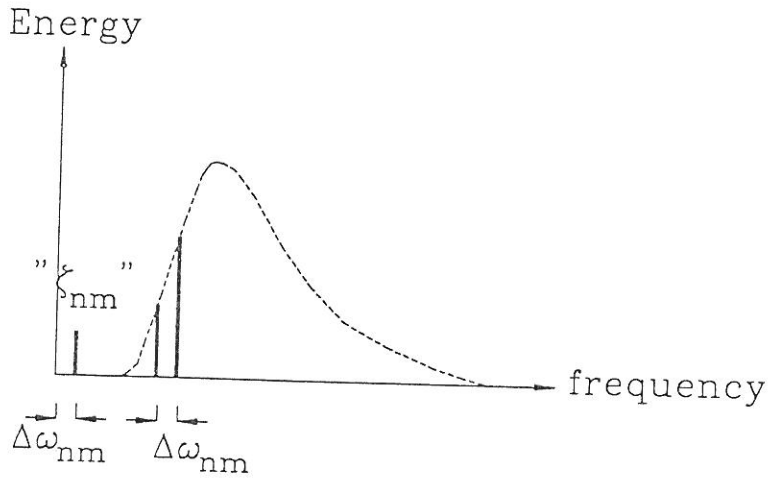

Figure 2.19: Calculation of second order correction term.

Frequency domain solution:

When waves are simulated in the frequency domain (i.e. when the Random Phase Method or Random Complex Spectrum Method is applied), the correct reproduction of group bounded long waves is obtained by superposition of the complex Fourier coefficients corresponding to the 1. and 2. order wave paddle displacement signals before performing InvFFT. The resulting wave paddle displacement signal will be correct to second order, and free long waves will therefore not exist.
Calculation of the second order correction corresponding to a certain frequency Δf_{nm} is illustrated in the figure below.

Time domain solution:

Consider a non-linear process $Y(t)$:

$$\mathrm{Y} = Y(t) = X(t) + \alpha X^2(t)$$

Remembering that α normally is frequency dependent $\alpha = \alpha(\omega_n, \omega_m)$, we can insert $X(t) = a_n cos(\omega_n t) + a_m cos(\omega_m t)$ and write the equation again:

$$\mathrm{Y} = a_n cos(\omega_n t) + a_m cos(\omega_m t) + \alpha \left[a_n^2 cos^2(\omega_n t) + a_m^2 cos^2(\omega_m t) + a_n a_m cos(\omega_n t) cos(\omega_m t) \right]$$

Reformulating the equation given above using the cosine relations we obtain:

$$
\begin{aligned}
Y = \; & a_n cos(\omega_n t) + a_m cos(\omega_m t) + && \textit{(linear terms)} \\
& \tfrac{1}{2}\alpha a_n^2 + \tfrac{1}{2}\alpha a_m^2 + && \textit{(offset)} \\
& \tfrac{1}{2}\alpha a_n^2 cos(2\omega_n t) + \tfrac{1}{2}\alpha a_m^2 cos(2\omega_m t) + && \\
& \tfrac{1}{2}\alpha a_n a_m cos((\omega_n + \omega_m)t) + && \textit{(2.order super harmonics)} \\
& \tfrac{1}{2}\alpha a_n a_m cos((\omega_n - \omega_m)t) && \textit{(2.order sub harmonics)}
\end{aligned}
$$

In the terminology of water waves the non-linear terms are named *Bounded Long Waves* (2.order sub harmonics), *Stokes 2.order Waves* (2.order super harmonics) and *2.order super harmonic waves* (2.order super harmonics).

An ordinary 2.order FIR filter will reproduce all the terms: Offset, 2.order super harmonics and 2.order sub harmonics given above.

The discrete frequency domain equation for a non-linear filter is:

$$G^*(\omega_n, \omega_m, \Delta\omega_{nm}) = H(\omega_n) \cdot F(\Delta\omega_{nm}) \cdot H(\omega_m)$$

where

G^*: Transfer function for filter in frequency domain
H, F: Two arbitrary functions (frequency domain)

This equation simply expresses that if G^* can be separated into the two functions H and F then the non-linear process is identically described by the process Y given above.

The *problem* with the FIR-filter is that it will generate all 2.order terms. In order to generate specified waves, i.e. bounded long waves, Stokes 2.order waves and 2.order super harmonic waves $\alpha(\omega_n, \omega_m)$ or in other words $H(\omega)$ and $F(\Delta\omega)$ must be found according to the requirements from the transferfunction.

In the case where only the bounded long waves is required the transfer function G^* must be *fitted* to the long wave transfer function. The frequency range and the Δfrequency range for the fitting must be controlled through the fitting algorithm in order to only have long waves.

The frequency range for H is the part of the wave spectrum with significant energy. The Δfrequency range for F is from zero to the frequency where energy starts to exist in the spectrum. For all other frequencies the values of H and F are zero.

When the filter coefficients are found the bounded long waves are added to the linear wave signal simply by filtering the linear wave signal through the filters *(Take linear*

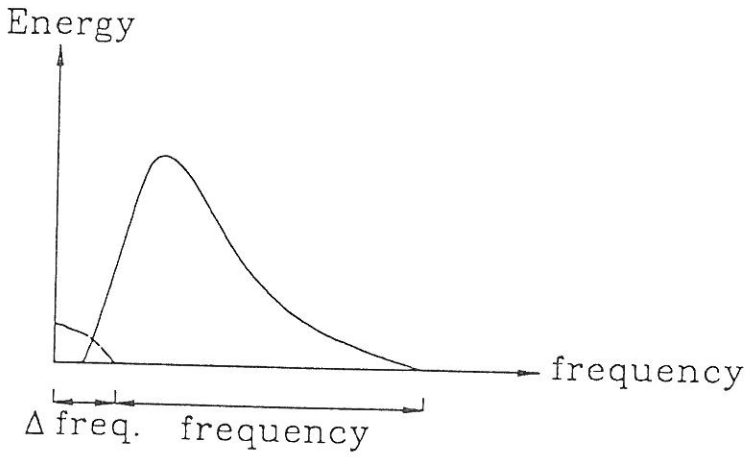

Figure 2.20: Frequency range for calculating *long wave* filters.

wave signal and convolve with H-filter, take result of convolution and convolve with F-filter).

2.8 References

Biesel, F., 1951.
Les Apparails Generateurs de Houle en Laboratorie.
La Houille Blanche, Vol. 6, nos. 2,4 et 5.

N. E. Ottesen-Hansen, 1978.
Long Period Waves in Natural Wave Trains.
Prog. Rep. 46, Aug. 1978, Inst. Hydrodyn. and Hydraulic Eng., DTH.

D. Nunes, 1981.
Random Wave Generation by Linear Digital Filtering of Gaussian White Noise
2nd Congress of I.M.A.E.M., Trieste.

Sand, S.E., 1982.
Long Wave Problems in Laboratory Models.
J. Wat. Ways, Port, Coastal and Ocean Div., ASCE 108(WW4).

H. Tuah and Robert T. Hudspeth, 1982.
Comparison of Numerical Random Sea Simulations.
Jour. of the Waterway, Port, Coastal and Ocean Div., Vol. 108, no. WW4.

John H. Karl, 1989.
An Introduction to Digital Signal Processing.
Academic Press, San Diego.

Fredsøe, J., 1990.
Hydrodynamik. (in danish)
Den private Ingeniørfond, DtH.

Chapter 3

3-D wave generation

From an engineering point of view the knowledge of the 3 dimensional structure of ocean waves is essential for: design of off-shore structures, estimating transport of marine sediment, ship motion and so forth. Hence, the generation of 3-D waves in laboratory facilities will be of interest when conducting scaled experiments concerning such topics.

Measurements in the ocean environment have founded the basis for several theoretical descriptions of the 3-D wave field. The directional wave spectrum, $S_\eta(f,\theta)$, is often considered a product of the uni-directional wave spectrum, $S_\eta(f)$, and a spreading function, $D(f,\theta)$. That is

$$S_\eta(f,\theta) = D(f,\theta)\cdot S_\eta(f) \tag{3.1}$$

where f is the wave frequency, θ the wave propagation angle and $D(f,\theta)$ must satisfy

$$\int_{-\pi}^{\pi} D(f,\theta)d\theta = 1 \tag{3.2}$$

to assure identical wave energy in $S_\eta(f,\theta)$ and $S_\eta(f)$.

Several semi-empirical proposals to the formulation of $D(f,\theta)$ have been reported and most suggestions consider D to be independent of the frequency. The *Cosine-power* or $\cos^{2s}$ spreading function, see Mitsuyasu (1975):

$$D(f,\theta) = \frac{s^{2s-1}}{\pi}\frac{\Gamma^2(s+1)}{\Gamma(2s+1)}cos^{2s}\left(\frac{\theta-\theta_0}{2}\right) \tag{3.3}$$

where s is a spreading parameter and Γ the Gamma function, was found to provide a reasonable fit to measured ocean wave spectra by Longuet-Higgins, Cartwright and Smith (1961) who used a frequency independent value of s.

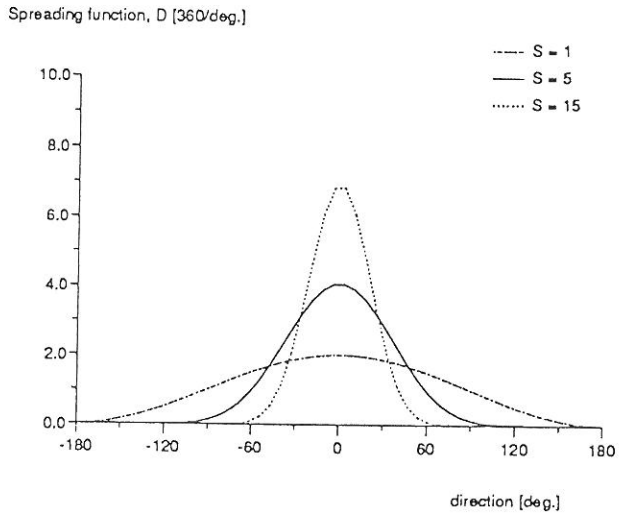

Figure 3.1: The spreading function, $D(f, \theta)$, for various constant values of the spreading parameter, s.

In Figure 3.1 D is plotted as function of θ for various values of s.

Mitsuyasu et al. (1975) have reported on extensive measurements of directional spectra and proposed the *Cosine power* spreading function to be applied with a frequency dependent s parameter. In their suggestion the variation of D exhibits the smallest degree of directional spreading, maximum s value, at frequencies near the peak frequency.

If the directional wave field is considered the sum of a number of wavelets with the elevation $\eta(x, y, t)$:

$$\eta(x, y, t) = a \cdot \cos(2\pi f t - kx \cos\theta - ky \sin\theta + \varphi) \tag{3.4}$$

where

a : the wave amplitude,
t : the time,
k : the wave number, $2\pi/L$,
(x, y) : the spatial coordinates and
φ : an arbitrary phase, uniformly distributed in $[-\pi; \pi[$.

Introducing the total wave energy of the wavelet, E_t, the amplitude can be rewritten:

$$a = \sqrt{\frac{2}{\rho g} E_t} \tag{3.5}$$

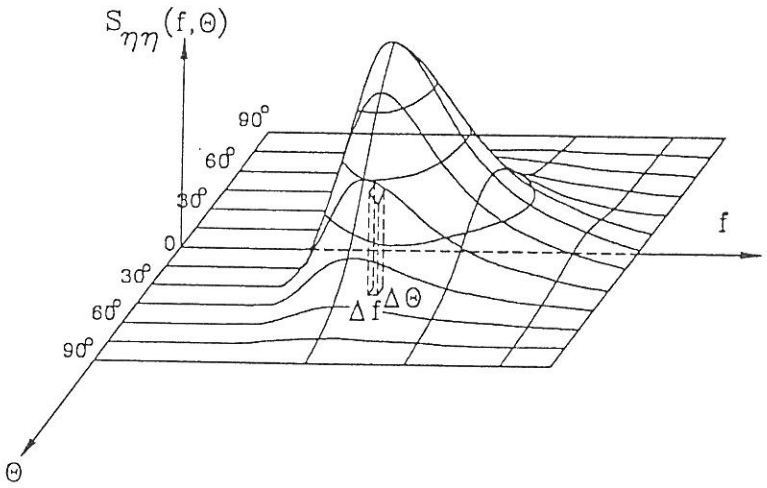

Figure 3.2: Energy 'packet' selection from a directional energy wave spectrum.

where ρ and g is the water density and gravitational acceleration ,respectively.

If the surface elevation is considered a Gaussian stochastic process characterized by a specified energy wave spectrum, S_η, sufficiently small $\Delta\theta$ and $\Delta\varphi$ can be chosen and the wave spectrum can be decomposed into a number of energy 'packets' each containing the approximate energy:

$$E_t \approx \rho g S_\eta(f,\theta)\Delta\theta\Delta f \tag{3.6}$$

Figure 3.2 illustrates the choice of such an energy 'packet'.

Combining the Equations 3.4 - 3.6 and letting $\Delta\theta$ and Δf decrease towards $d\theta$ and df, respectively, the total surface elevation can be written as

$$\eta(x,y,t) = \int_0^\infty \int_{-\pi}^{\pi} \sqrt{2S_\eta(f,\theta)d\theta\ df}\cos(2\pi ft - kx\cos\theta - ky\sin\theta + \varphi) \tag{3.7}$$

The integral in Equation 3.7 is often referred to as a pseudo-integral, referring to its lack of mathematical stringency. In any way it is a descriptive way to symbolize the limiting processes, $\Delta\theta \to d\theta$ and $\Delta f \to df$.

3.1 3-D Biésel transfer function

In Section 2.1 the Biésel transfer function for uni-directional linear waves, F_2, was calculated for various types of generator systems. To generate oblique linear waves

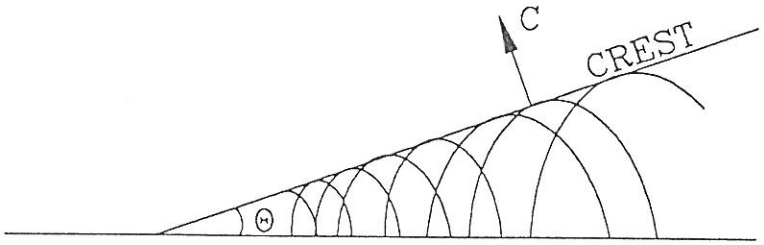

Figure 3.3: Huygens' principle in generating oblique waves. Regular wave travelling in the θ-direction.

travelling in a direction different from the x-axis direction perpendicular to the front of the generator, a different transfer function, F_3, must be applied.

Consider a wave generating system where the generator front consists of a number of very small paddles. A oblique regular wave can then be generated using Huygens' principle, by introducing a suitable delay between the wave paddles as illustrated in Figure 3.3. Each wave paddle moves harmonically in the x-axis direction with the amplitude x_a. It is evident that the required delay of the individual wave paddles will lead to a sinusoidal shape of the front of the wave generator. If the front of the actual wave generating system fails to reproduce this shape correctly, as always will be the case due to the finite width of the wave paddles, undesired waves will be generated. In Section 3.4 these so-called spurious waves are discussed. If the wave length of the generated wave is L the wave length from maximum to maximum of the sinusoidal front of the wave generator, $l = L/\sin\theta$. The delay, φ_p, between neighbouring wave paddles of width l_p is $l_p \cdot 2\pi/l$, or more convenient

$$\varphi_p = l_p \cdot \frac{2\pi \sin\theta}{L} \tag{3.8}$$

Consider a small part of the wave generator, say of the length Δl, and let the generated regular wave travel in the θ direction with the group celerity, c_g. See Figure 3.4.

The energy flux, E_f, in the generated oblique wave over the length $\Delta l \cdot \cos\theta$ in Figure 3.4 is

$$E_f \sim a^2 \cdot c_g \cdot \Delta l \cos\theta \tag{3.9}$$

where a is the wave amplitude and θ the direction of travel. Assuming that no energy is transported along the crest of the generated wave, this energy flux must be balanced by the energy flux over the length Δl just in front of the wave paddle.

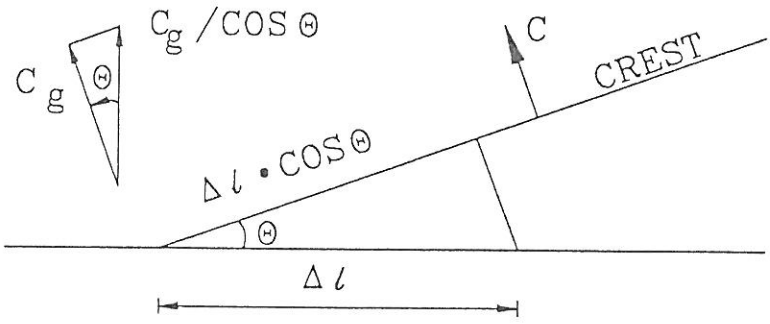

Figure 3.4: Small part of wave generator, generating a oblique regular wave.

As the wave amplitude in front of the paddle is $x_a \cdot F_2$, and the corresponding group velocity is $c_g/\cos\theta$, this energy flux can be written

$$E_f \sim (x_a \cdot F_2)^2 \frac{c_g}{\cos\theta} \Delta l \tag{3.10}$$

Combining Equation 3.9 and 3.10 the amplitude in the generated oblique wave, a, equals $x_a \cdot F_2/\cos\theta$ and consequently the 3-D Biésel transfer function

$$F_3 = F_2/\cos\theta \tag{3.11}$$

Hence, by decomposing a specified directional wave spectrum into a number of wavelets of the form given in Equation 3.4, the wave paddle displacement necessary for generating the individual wavelets can be calculated using the transfer function given in Equation 3.11 and the delay between the wave paddles can be calculated using Equation 3.8. By superposition the total paddle displacement can then be obtained.

3.2 Generating oblique 2-D waves

The methods for generating 2-D waves perpendicular to the wave generators described in Chapter 2

- Random Phase Method
- Random Complex Spectrum Method
- White Noise Filtering Method

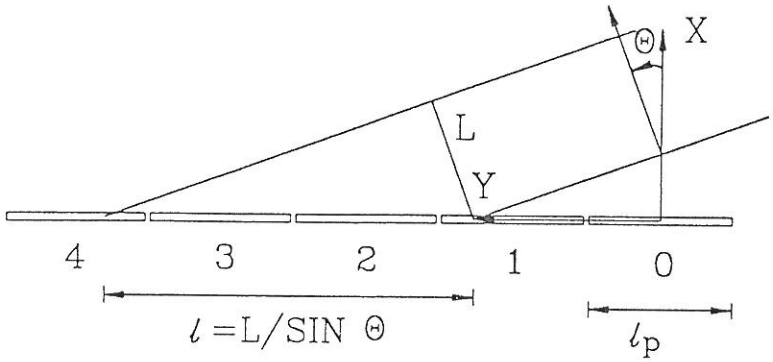

Figure 3.5: Wave generating system with segmented wave paddles. Definition sketch

are applicable when generating oblique 2-D waves as well. Basically the paddle displacement for one paddle, say the 0th, is calculated using one of the methods from Chapter 2 and the displacement for the ith paddle is calculated by introducing an appropriate delay, φ_{pi}, relative to the displacement of the 0th paddle.

Consider a wave generator system consisting of n segmented wave paddles with the width l_p. A coordinate system is introduced as illustrated in Figure 3.5.

If the wave paddle displacement is calculated for a regular wave with the wave length L travelling in the x-axis direction, the delay between the ith and the 0th wave paddle when generating the same regular wave travelling in the θ-direction, see Equation 3.8, is

$$\varphi_{pi}(f) = i \cdot l_p \frac{2\pi \sin\theta}{L(h,f)} \tag{3.12}$$

As the paddle displacement must be calculated using the 3-D Biésel transfer function from Equation 3.11 the calculated 2-D displacement must be multiplied by $\cos\theta$.

3.2.1 Random Phase and Random Complex Spectrum Methods

Both methods involve an inverse Fourier transform of calculated Fourier coefficients for the discrete paddle-displacement energy spectrum, $\sigma_x^2(f_j)$:

$$\begin{aligned} A_j &= a_j \cdot \cos\varphi(f_j) \\ B_j &= a_j \cdot \sin\varphi(f_j) \end{aligned} \tag{3.13}$$

where $a_j = \sqrt{\sigma_x^2(f_j)/2}$ to produce the displacement of the wave paddle.

In the Random Complex Spectrum Method $\cos\varphi(f_j)$ and $\sin\varphi(f_j)$ are replaced by two random Gaussian variables with zero mean and $\sigma = 1$. This, however, does not affect the general principle in the following.

For each pair of frequency components the delay is introduced by substituting $\varphi(f_j)$ in 3.13 by $\varphi(f_j) - \varphi_{pi}(f_j)$. Using the trigonometric addition formulas, and assuming that a_j is calculated using the 2-D Biésel transfer function derived in Chapter 1, the modified Fourier coefficients for the discrete paddle-displacement energy spectrum are:

$$\begin{aligned} A_{ij} &= a_j \cdot \cos\theta(\cos\varphi(f_j)\cos\varphi_{pi}(f_j) + \sin\varphi(f_j)\sin\varphi_{pi}(f_j)) \\ B_{ij} &= a_j \cdot \cos\theta(\sin\varphi(f_j)\cos\varphi_{pi}(f_j) - \cos\varphi(f_j)\sin\varphi_{pi}(f_j)) \end{aligned} \tag{3.14}$$

Performing inverse Fourier transform on the n sets of Fourier coefficients in Equation 3.14 leads to the appropriate displacement time series for each of the n wave paddles.

3.2.2 White Noise Filtering Method

The White Noise Filtering Method involves the use of two filter operators:

The first filter operator, the Surface Elevation filter, is calculated by performing inverse Fourier transform on a discrete frequency response function corresponding to the target wave energy spectrum. Convolved with a white noise signal the Surface Elevation filter produces the appropriate surface elevation time series.

The second filter operator, the Biésel filter, is calculated by performing inverse Fourier transform on a discrete frequency response function corresponding to the inverse of the far field Biésel transfer function from Chapter 1. Convolved with the surface elevation the Biésel filter produces the corresponding wave paddle displacement time series.

To generate oblique 2-D waves using the White Noise Filtering Method the approach described in the previous section can be used to calculate appropriate Biésel filter coefficients for each of the n wave paddles. Consequently to generate oblique 2-D waves the 2-D discrete frequency response function for the Biésel filter:

$$\begin{aligned} H(f_j).re &= \cos(\Phi)\frac{1}{K_f(f_j)} \\ H(f_j).im &= \sin(\Phi)\frac{1}{K_f(f_j)} \end{aligned} \tag{3.15}$$

where K_f is the far field Biésel transfer function, must be modified to apply to the ith wave paddle:

$$\begin{aligned} H(f_j).re &= \frac{\cos\theta}{K_f(f_j)}(\cos\Phi\cos\varphi_{pi}(f_j) + \sin\Phi\sin\varphi_{pi}(f_j)) \\ H(f_j).im &= \frac{\cos\theta}{K_f(f_j)}(\sin\Phi\cos\varphi_{pi}(f_j) - \cos\Phi\sin\varphi_{pi}(f_j)) \end{aligned} \tag{3.16}$$

Performing inverse Fourier transform on the n frequency response functions in Equation 3.16, the Biésel filters for each of the n wave paddles are obtained. Convolved with the surface elevation time series, calculated by convolving the Surface Elevation filter with a white noise signal, these filter operators produces the appropriate displacement time series for each of the wave paddles.

3.3 Generating irregular 3-D waves

Directional irregular waves can be expressed as a linear superposition of a large number of wavelets of the type shown in Equation 3.4, with frequency f, propagation direction θ, wave length L, and phase φ. Thus, a simultaneous generation of a number of oblique linear waves enables a reproduction of a directional wave field in a laboratory wave basin.

Two in principle different models are available when generating input signals for 3-D wave systems:

- Single summation model:
  In this model a single direction is assigned to each frequency component. Consequently the double pseudo-integral, Equation 3.7, is represented by a single summation leading to a paddle displacement for the ith wave paddle, x_i:

$$x_i(t) = \sum_{j=1}^{N\cdot M} \frac{b_j}{F_3(f_j,\theta_j)} \cos(2\pi f_j t - \varphi_{pi}(f_j,\theta_j) + \varphi(f_j)) \tag{3.17}$$

  where

$$b_j = \sqrt{2S_e ta(f_j)\Delta f} \quad ,$$

$$F_3(f_j,\theta_j) = \frac{F_2(f_j)}{\cos\theta_j} \quad \text{and}$$

$$\varphi_{pi}(f_j,\theta_j) = il_p\frac{2\pi\sin\theta_j}{L(h,f_j)}$$

in which $F_2(f_j)$ is the 2-D Biésel transfer function given in Chapter 1.
For the method to be successful the choise of θ_j must represent the adopted directional spreading function, $D(f,\theta)$. This is often achieved by picking θ_j as a random number with a propability density function equal to $D(f,\theta)$.

- Double summation model:
In this model multiple directions are assigned to each frequency component. The paddle displacement of the ith paddle can then be written:

$$x_i(t) = \sum_{j=1}^{N}\sum_{k=1}^{M} \frac{b_{jk}}{F_3(f_j,\theta_k)} \cos(2\pi f_j t - \varphi_{pi}(f_j,\theta_k) + \varphi(f_j,\theta_k)) \qquad (3.18)$$

where

$$b_j = \sqrt{2S_e ta(f_j,\theta_k)\Delta f \Delta\theta} \quad ,$$

$$F_3(f_j,\theta_k) = \frac{F_2(f_j)}{\cos\theta_k} \quad \text{and}$$

$$\varphi_{pi}(f_j,\theta_k) = il_p \frac{2\pi \sin\theta_k}{L(h,f_j)}$$

in which θ_k often simply is chosen equally distributed from $-\frac{\pi}{2}$ to $\frac{\pi}{2}$.

A specific problem relates to the double summation model. The phase difference between two wavelets with equal frequencies but different propagation directions does not vanish in the cross spectra. The phenomenon, known as phase locking, results in different spectral properties of the generated irregular wave field dependent on the spatial coordinates. Consequently, the irregular surface is non-ergodic. To reduce this effect the number of wave components in the double summation model, $N \cdot M$, must be increased significantly relative to the number of components in the single summation model, $N \cdot M$. Takayama et al. (1989) conclude that the required number of wave components in the double summation model must be 20 times larger than in the single summation model to obtain the same quality of the generated wave field. Therefore several authors generally advocate the single summation model for laboratory use, simply to reduce computation time. In some generation methods, however, the double summation model can be attractive in order to avoid, for example, inverse Fourier transform of very long arrays.

In the following generation methods only the single summation model will be discussed, but the applicability to a double summation model is straight forward and will briefly be described.

Consider a wave generation system with n segmented wave paddles and coordinate system as outlined in Figure 3.5.

3.3.1 Inverse Fourier Transform methods

The two Inverse Fourier Transform methods for generating irregular 2-D waves described in Chapter 2:

- Random Phase Method
- Random Complex Spectrum Method

The single summation model is applied using a technique very similar to the method for generating oblique 2-D waves, as described in Section 3.2.

Calculating the discrete wave energy spectrum, $\sigma_\eta^2(f_j) = S_\eta(j \cdot \Delta f)\Delta f$, the $N \cdot M$ frequency components for the ith wave paddle can be calculated by picking appropriate propagation directions, θ_j, using the techniques described in the previous section, and random phases, $\varphi(f_j)$ equally distributed from 0 to 2π:

$$\begin{aligned} A_{ij} &= \frac{b_j}{F_3(f_j,\theta_j)}(\cos\varphi(f_j)\cos\varphi_{pi}(f_j,\theta_j) + \sin\varphi(f_j)\sin\varphi_{pi}(f_j,\theta_j)) \\ B_{ij} &= \frac{b_j}{F_3(f_j,\theta_j)}(\sin\varphi(f_j)\cos\varphi_{pi}(f_j,\theta_j) - \cos\varphi(f_j)\sin\varphi_{pi}(f_j,\theta_j)) \end{aligned} \quad (3.19)$$

where $b_j = \sqrt{\sigma_\eta^2(f_j)/2}$.
Using the Random Complex method $\cos\varphi(f_j)$ and $\sin\varphi(f_j)$ are replaced by two random Gaussian variables as described in Chapter 2.

Performing inverse Fourier Transform on the n set of $N \cdot M$ Fourier coefficients in Equation 3.19 will lead to the appropriate displacement time series for each of the n wave paddles.

A double summation model could be applied by calculating M discrete wave energy spectra, $\sigma_{eta}^2(f_j,\theta_k) = S_\eta(j\cdot\Delta f, k\cdot\Delta\theta - \frac{\pi}{2})\Delta f\Delta\theta$, and creating M set of N frequency components for each of the n wave paddles, performing inverse Fourier Transform and superpositioning the M displacement time series for each of the wave paddles.

3.3.2 White Noise Filtering methods

The method described below is strichtly following the equivilent method described in Chapter 2:

- White Noise Filtering Method

Consequently, the Biésel filter and the Surface Elevation filter could be combined when generating 3-D irregular waves, if not the surface elevation time series are of any use, for example for calculating bounded sub or super harmonic waves, as discussed in Chapter 2. If not the two filters are combined only the Biésel filter needs to be modified for generating irregular 3-D waves.

In a single summation model a Biésel filter for each of the n wave paddles must be designed. In alignment with the previous section and Section 2.2 it is easily recognized that the frequency response function for the 3-D Biésel filter assigned to the ith wave paddle can be calculated as:

$$\begin{aligned} H(f_j).re &= \frac{1}{F_3(f_j,\theta_j)}(\cos\Phi\cos\varphi_{pi}(f_j,\theta_j)+\sin\Phi\sin\varphi_{pi}(f_j,\theta_j)) \\ H(f_j).im &= \frac{1}{F_3(f_j,\theta_j)}(\sin\Phi\cos\varphi_{pi}(f_j,\theta_j)-\cos\Phi\sin\varphi_{pi}(f_j,\theta_j)) \end{aligned} \tag{3.20}$$

where $\varphi_{pi}(f_j,\theta_j)$ and $F_3(f_j,\theta_j)$ are defined in the previous section and $\Phi=-\frac{\pi}{2}$.

Performing inverse Fourier Transform on the n frequency response functions in Equation 3.20 the Biésel filters for each of the wave paddles are obtained. Convolved with the surface elevation time series these filter operators produce the appropriate displacement time series for each of the wave paddles.

If the two filters, the Surface Elevation filter and the Biésel filter, are to be combined, this is achieved by creating a frequency response function consisting of the components from the Biésel frequency responce function multiplied by the complex conjugate of the corresponding components in the Surface Elevation frequency response function, that is $H(f_j,\theta_j)=H_B(f_j,\theta_j)\cdot H_S^*(f_j,\theta_j)$, and performing inverse Fourier Transform to obtain the filter operators. A double summation model can be applied by creating M filters for M different directions for each of the n wave paddles. By convolving M white noise arrays with each of the directional filters and sum up for all directions the n paddle displacements are calculated.

3.4 Spurious waves and other laboratory difficulties

Generating laboratory waves using a truncated segmented paddle system will generally affect the quality of the generated wave field. Due to the in-capability of the segmented front of the wave maker to form a perfect sinusoid the principles outlined in Section 3.1 and 3.2 are not completely valid. The effect is dependent on the wave length L, the propagation direction θ and the paddle width l_p, for

example expressed as the ratio $l/l_p = L/(l_p \sin\theta)$, and two fold:
Incorrect energy is feed into the generated waves because the integrated variance of the actual displacement of the wave paddle front is different from that of a ideal sinusoidal displacement.
Incorrect directed energy is feed into the generated waves causing spurious waves, travelling in directions different from the main waves, to be generated.
Both effects cause the actual transfer function between the stroke of the wave paddle and the wave height to be different from the theoretical 3-D Biésel transfer function F_3. Reference can be made to Sand (1979) for a detailed description of the phenomena and usefull implementations into a specified wave generating system.

Other effects are

- The truncation of the wave maker causes diffraction, that is wave energy travelling along the wave crest and, consequently, reducing the height of the generated wave.
- The truncation of the wave basin causes reflection from the side walls which, consequently, affects the directional spreading of the wave field.

These effects significantly reduce the horizontal area inside which the specified wave field is generated.

3.5 References

Longuet-Higgins, M.S., D.E. Cartwright, and N.D. Smith, 1961.
Observations of the directional spectrum of sea waves using the motions of a floating buoy.
In *Ocean Wave Spectra*, Prentice-Hall, pp. 111-132.

Mitsuyasu, H, et al., 1975.
Observations of the directional spectrum of ocean waves using a cloverleaf buoy.
In *Journal of Physical Oceanography*, Vol. I, pp. 750-760.

Sand, S.E., 1979.
Three-Dimensional Deterministic Structure of Ocean Waves
PhD thesis from The Technical University of Denmark.

Takayama, T., T. Hiraishi, and Y. Goda, 1989.
Comparison of single and double summation models for multi-directional wave generation.

In *Proc. International Association for Hydraulic Research XXIII Congress* Ottawa, Canada, August 21-25.

Chapter 4

The PC enviroment

This chapter describes the interface between software and PC I/O-ports. The describtion is closly related to Data Translations products AD/DA-board DT2811 and DA-board DT2815 which are used by the wave generation software package PROFWACO.

In addition, an introduction to the multitasking concept and the *build-in* real time facillities in PROFWACO is given.

4.1 DA-conversions

PC based controlling is comprised of digital logic, computer architecture, signal conversion technology, analog circuitry and software. This section briefly explains some of the key specifications and concepts needed in the design of an I/O system.

Generally, I/O systems can be based on digital technology or on analog technology. Both technologies have advantages. The following chapter describes an analog system.

Output resolution is usually specified in *bits*. The majority of available products currently offer 12-bits resolution, though 8-, 10-, 14- and 16-bits resolution products are available. The conversion from bits of resolution to actual resolution is given by: actual resolution $= 2^{bits\ resolution}$. The DT2811-board and the DT2815-board are 12-bits cards which have a actual resolution of 4096.

Output range is normally ± 5.0 volt in bipolar mode. This means that a servo-loop must be designed to use the whole output range in order to have maximum resolution. The resolution in volts is the ratio of the total output range to actual resolution, i.e. 10 volt / 4096 DA-steps = 2.44 millivolt/DA-step.

Maximum update rate (throughput) is specified in samples/second. Most multi-channel DA-boards consist of a single DA converter and output multiplexer. The multiplexer acts as a switch that allows output signal to each of the channels to be send independently. To find the maximum update rate per channel, the maximum update rate for the DA-converter must be divided by the number of channels. The settling time of the DA-converter is the time for one DA conversion. Note that the output from one channel to the next channel will be delayed by at least one settling time.

Timers on the DA-board are used to set accurately the update rate of the analog output. If no timer is available on the DA-board the internal clock in the PC can be used.

The PC/AT bus is often referred to as the ISA bus (Industry Standard Architecture). The ISA bus performs 16-bit transfer and can perform up to 300 k transfers per second. The DT2811-board and the DT2815-board are especially designed to plug into the ISA bus in a IBM compatible PC.

The servo controller is used to amplify signal to wave maker. It is possible to have a *displacement* controled servo loop, a *velocity* controlled servo loop or a combination of both. The servo loop can be analog or digital. The servo loop can even be included in the PC leading to a rather complex system.

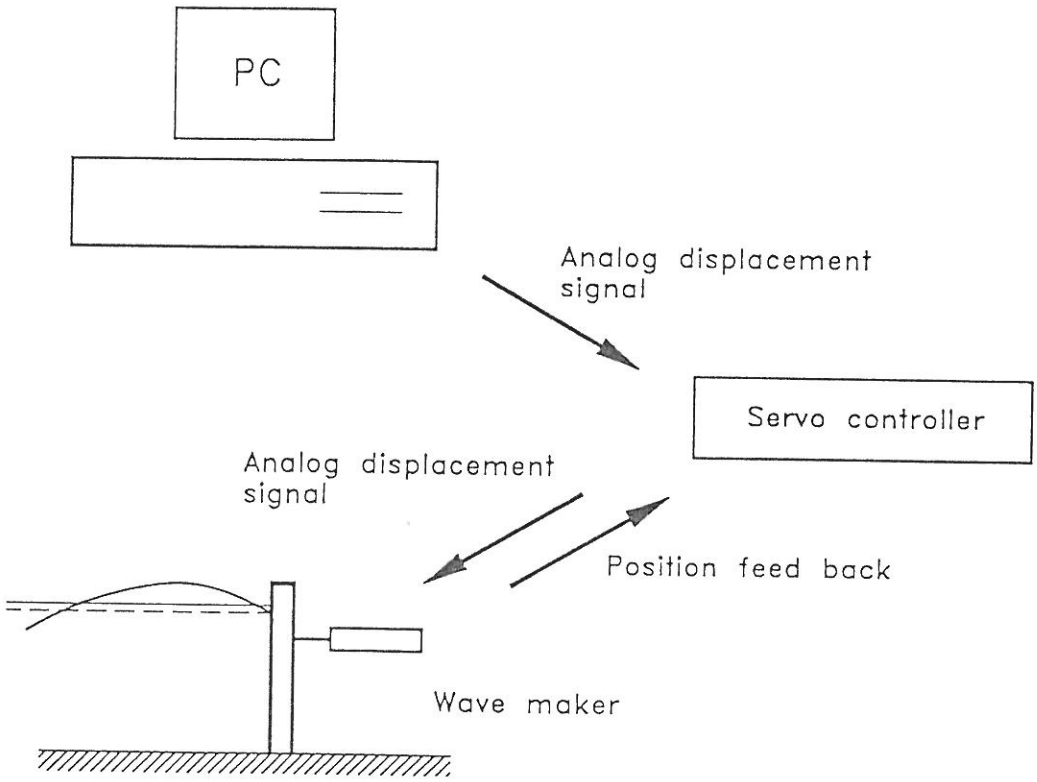

Figure 4.1: *Example of controlling system.*

PROFWACO is intended for a *displacement* controlled analog servo system with a control signal ranging from - 5.0 volt to + 5.0 volt. In this case the PC must be able to send different analog signals to every wave maker. For that use Data Translation DA-board DT2815 or Data Translation AD/DA-board DT2811 is used. Both IO-boards have 12 bits resolution.

For each output operationry I/O the user must : Transfer data from RAM to DA-board Data Register, Address Multiplexer, start conversation and eventually check the Status register on completion of the operation.

The DT2811-board has 2 DA-channels reducing its applicability to 2-D wave generation. The DT2815-board is equiped with 8 DA-channels which for most 3-D wave basins are too few channels. If more than one DT2815-boards are installed into the same PC the baseaddresses of the boards must be different.

4.2 Real-time programming

Real-time programming is considered to be an upper level of normal sekvential programming. The essence of real-time application systems is the ability to process numerous events occuring seemingly random in time. These events are *asynchronous* because they can occur at any time, and they are potentially *concurrent* because one event might occur while another is beeing processed.

Any single program that attemps to process multiple, concurrent, asynchronous events is bound to be complex. The program must perform several functions. It must process the events. It must remember which events have occured and the order in which they occured. It must remember which events have occured but have not been processed.

There are two ways that computer systems can schedule processing associated with detecting and controlling events - polling and interrupt processing.

Polling is implemented by having the software periodically check to see if certain events have been requested. An example of polling from a human perspective can be created using a class of students and a teacher. If the teacher rather than spotting raised hands, asks specially each student in the class wheather the student has any quistions, then the teacher is polling the students. Polling has a major shortcomming: a significant amount of the processor time is spent testing to see if events are requested. If events are not requested, the processor time has been wasted.

Interrupt processing is the second method of process controlling. When an event occurs the processor is literally interrupted. Rather than executing the next sequential instruction, the processor begins to execute a task associated specially with the detected event.

The classroom example used earlier to portray polling can also be used to illustrate interrupt processing. If a student has a quistion, he raises his hand and speaks the teatchers name. The teacher, interpreting this as an interrupt, finishes his sentence and deals immediately with the students quistion. After the teacher has answered the student he returns to what he was doing before he was interrupted.

Interrupts are divided into two types because of the different role they play for the control of software and hardware. The two ways of activating the interrupt routines are: software interrupt and hardware interrupt .

A software interrupt is an interrupt activated by a special assembly language

instruction, the INT instruction. The INT instruction is always used in conjunction with the number of the interrupt to be executed. This allows a program to call a routine even when the exact address of the routine is unknown, but the program knows that the routine is accessible as a interrupt routine. The routines in the ROM-BIOS and DOS kernel can be accessed by any program using interrupts this way. Simple routines like character input/output can be called directly from the ROM-BIOS and DOS kernel without having to worry about the memory address and structure of the routine.

A hardware interrupt comes directly from a hardware component of the system such as the keyboard, the disk drive or the internal clock. The hardware devices use one of the interrupts from $08 to $0F, and the proper interrupt is executed when a device wants to get the processors attention. As with software interrupt, the corresponding interrupt routine is then called. The address of this routine is obtained from the interrupt vector table. The interrupt vector table specifies the interrupt and the location (starting address) of its interrupt routine in memory.

There are two types of hardware interrupts, those that can be suppressed and those that cannot be suppressed. Writing to disk, for example, is a *maskable interrupt* that can be suppressed with the assembly language instruction CLI (Clear Interrupt Flag). This means that the interrupt call will not be executed and that writeing on disk cannot be done until the suppression is lifted with the STI instruction (Set Interrupt Flag).

Hardware interrupts originating from one of the processors on the motherboard are often called internal hardware interrupts. The timer interrupt, which is executed at regular intervals to allow time measurements, is an example from this category.

Interrupt $08 is the timer interrupt which normally is called 18.2 times/second. Interrupt $08 is originally designed to run the internal clock in the PC. In all PC's the ocillator of the system timer has a frequency of 1.19318 MHz. On each cycle, the timer chip decrements the value in a internal 16-bit counter. When the ROM BIOS initializes the system timer, it stores a countdown value of 0 in the count register (memory address $40). This means that the timer chip decrements the counter 2^{16} times between pulses so interrupt occur 1193180/65536 = 18.2 times/second. Changing these register values it is possible to modify the update rate for interrupt $08.

It is possible to *steal* the interrupt, in such a way that instead of updating the internal clock it will call a user specified routine. This routine can, as an example, transfer data to the DA-cards. The interrupt $08 also issues software interrupt $1C, which can be used in programs that want to be notified when a system timer

tick occur.

4.3 References

Tischer, Michael 1990.
Turbo Pascal Internals. Data Becker, West Germany.

Manuals for the iRMX86 operating system.
Intel Corporation, California, USA, 1982.

DT2811 User Manual
Data Translation inc. 1987.

DT2815 User Manual
Data Translation inc. 1987.